Journal of Colloid and Interface Science 556 (2019) 140–146

Contents lists available at ScienceDirect

Journal of Colloid and Interface Science

journal homepage: www.elsevier.com/locate/jcis

Noble copper-silver-gold trimetallic nanobowls: An efficient catalyst

Krishna Kanta Haldar [a,*], Swati Tanwar [b], Rathindranath Biswas [a], Tapasi Sen [b], Jouko Lahtinen [c]

[a] Department of Chemical Sciences, School of Basic and Applied Sciences, Central University of Punjab, 151001 Bathinda, Punjab, India
[b] Institute of Nano Science and Technology, 160062 Mohali, Punjab, India
[c] Department of Applied Physics, Aalto University School of Science, FI-00076 Aalto, Finland

GRAPHICAL ABSTRACT

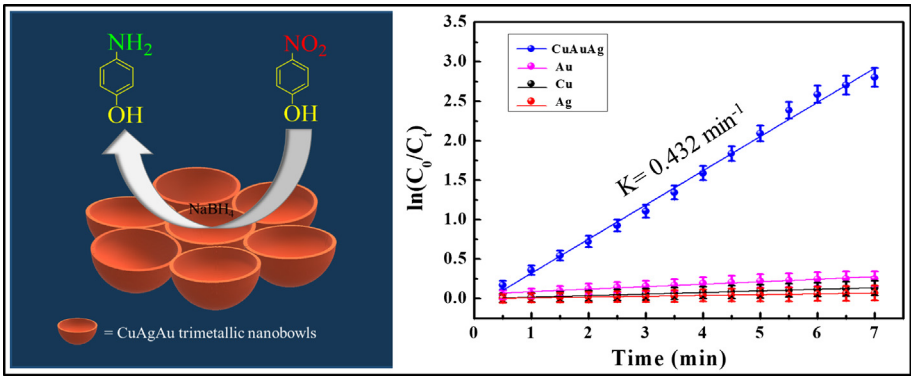

ARTICLE INFO

Article history:
Received 30 January 2019
Revised 12 August 2019
Accepted 12 August 2019
Available online 13 August 2019

Keywords:
Trimetallic
CuAgAu
Nanobowls
4-Nitrophenol
Catalyst

ABSTRACT

We demonstrated the design of tiny bowls of copper-silver-gold (Cu-Ag-Au) alloy type noble trimetallic nanocrystals with a unique shape. All the structural characterizations confirm the presence of copper (Cu), silver (Ag), and gold (Au) in the trimetallic nanobowls. Finally, we examined the catalytic efficiency of trimetallic Cu-Ag-Au nanobowls for reduction of 4-nitrophenol to 4-aminophenol and found that these nanobowls were 14, 23 and 43-fold more active than each of the constituent metals, Au, Cu and Ag, respectively.

1. Introduction

Multicomponent noble metal nanostructures have received much attention because of their fascinating electronic, optical, and catalytic properties as well as their excellent chemical stability [1–8]. Various types of metallic hetero-nanostructures with specific morphologies such as nanoalloys, nanorods, hollow, and core-shell type structures with enhanced physicochemical properties shave been found to be promising systems for diverse applications ranging from materials science to biology [9–12]. Among these nanostructures, the bimetallic nanostructures composed of platinum (Pt)/palldium (Pd) and gold (Au) [13] or silver (Ag) and Au have attracted much interest for their plasmonic, catalytic and sensor-based applications [14–17]. However, the high cost of these noble metals (e.g., Au and Pt) is a major limitation for the commercial development of noble metal catalysts. To date, enormous efforts

* Corresponding author.
E-mail address: cskkh@cup.ac.in (K.K. Haldar).

https://doi.org/10.1016/j.jcis.2019.08.047
0021-9797/

have been made to identify alternative catalysts including alloying Au with non-noble metals such as copper (Cu), cobalt (Co), Iron (Fe) and tin(Sn). Weiner at al. [18] reported the synthesis and detailed structural characterization of trimetallic nanocrystals using seed-mediated co-reduction methods. Patra et al. [19] prepared monodispersed Au-Cu-Sn trimetallic nanocubes and explored them for hydrazine oxidation. They also demonstrated thatthis trimetallic nanocube showed superior catalytic activity as compared to their constitutional counter metals. Further, Sun et al. [20] have shown that the designing of Au/Cu-Pt core/shell is indeed effective for optimizing nanoparticles catalysts for oxygen reduction as well as methanol oxidation reaction. Jing et al. [21] designed branched Pd and Pd-based trimetallic nanocrystals which are highly open structures suitable for methanol electro-oxidation when compared totheir constituent metals. Mao et al. [22] reported an efficient route for the synthesis of branched Pt-Pd-M (M = Co or nickel [Ni]) trimetallic nanocrystals via one pot.

However, most of the efforts have been made in combining Au with metals such as Pt, Pd, Cu, Fe, and Sn in alloy or core-shell type structures [23–26]. Here, we developed a solution based trimetallic nanocrystal with a unique bowl shape. The nanobowls have cavities of a few nanometers, which may hold small molecules such as 4-nitrophenol (4-NP). The fabricated trimetallic nanobowls are composed of the plasmonic Cu, Ag, and Au and their efficiency as acatalyst for reduction of 4NP to 4-aminophenol (4-AP) model reaction has been demonstrated in the present study. In almost all synthesized trimetallicCu-Ag-Au nanobowls nanostructures, Cu, Ag and Au metals were mixed homogeneously to form an alloy and spread out two-dimensionally. To the best of our knowledge, such trimetallic bowl-like Cu-Ag-Au nanostructures have not been explored previously for the reduction of 4-NP to 4-AP. This approach may be adapted to other multimetallic nanomaterials systems which will enable researchers to tune nanocrystal-based catalysis for various chemical reactions.

2. Experimental methods

2.1. Materials

Gold (I) chloride (Sigma Aldrich, 99.9%), silver nitrate (Qualikems, 99.9%), oleylamine (Sigma-Aldrich, Technical 70%). Copper dichloride dihydrate (98%), ethylene glycol (99%), 4-nitrophenol (98%) and sodium borohydride ($NaBH_4$, 97%) were purchased from LobaChemie. All the chemicals were used as received without further purification.

2.2. Synthesis procedure

The trimetallic noble Cu-Ag-Au based nanocrystals were synthesized in an aqueous medium under a mild condition in the presence of ethylene glycol and oleylamine. Briefly, 1.7 mL oleylamine, 5.3 mL ethylene glycol, and 23 mL of double distilled water were taken in a 100 mL three-neck round-bottle flask and the solution was sonicated until the mixture became completely transparent. Then, 2 mL of 100 mM copper dichloride aqueous solution was added to the mixture with slow stirring followed by addition of 0.004 g $NaBH_4$, stirring was continued for another 15 min at room temperature. The solution mixture was subsequently heated in an oil bath at 125 °C followed by the addition of 250 μLof 30mM gold (I) chloride and 2 mL of 30 mM silver nitrate. After 40 min the solution turned dark brown and then the heating was stopped and allowed to cool at room temperature. The product was purified several times with ethanol/acetone and centrifugation at 7000 rpm for 5 min. The precipitated trimetallic nanocrystals were dispersed in distilled water for further characterization using UV–vis spectrophotometry, transmission electron microscopy (TEM), X-ray diffraction (XRD), and X-ray photoelectron spectroscopy (XPS). Further, the catalytic activity of the synthesized nanocrystals were analyzed in the reduction of 4-NP to 4-AP model reaction following our earlier work [5].

3. Results and discussion

3.1. Structural characterisation

The Cu-Ag-Au trimetallic nanocrystals were synthesized in aqueous medium under mild conditions. As Cu, Ag and Au nanostructures show optical absorption, the reactions were monitored spectrophotometrically with a UV–vis spectrophotometer (Shimadzu UV-2450). Absorption spectra were obtained at different reaction times at room temperature in order to understand the formation of the trimetallic nanocrystals (Fig. 1a[i–iv]). The plasmonic absorbance band centered at ~430 nm was observed due to pure Ag nanoparticle [27] (Fig. 1a, curve i) and the band at ~520 nm represented pure Au nanoparticle [28,29] (Fig. 1a, curve ii). The peak at 620 nm observed at the initial reaction time points represented Cu nanoparticles (Fig. 1a, curve iii). Within 10 min of reaction, a clear absorption band at ~552 nm with a small hump at ~450 nm was observed due to the formation of the Cu-Ag-Au trimetallic structures (Fig. 1a, curve iv). It is reported that the surface plasmon resonance band (SPR) of Cu nanoparticles undergo a gradual damping upon oxidation and formation of an oxide layer outside Cu nanoparticles [30–34]. The shift of the band edge absorption compared to its constituent metals reflects the growth of Cu-Ag-Au trimetallic nanostructures.

Fig. 1b represents typical high resolution bright field TEM images of the monodispersity Cu-Ag-Au trimetallic nanocrystals synthesized in our optimized reaction condition, which show a tiny bowl-like structure. Without size sorting, the Cu-Ag-Au trimetallic nanocrystals showed good monodispersity and were mostly uniform in shape. Fig. 1c shows an inverted view of the TEM image of the synthesized trimetallic Cu-Ag-Au nanocrystals. The high magnification inverted TEM image further confirmed the three-dimensional bowl-like structure of the Cu-Ag-Au nanocrystals with a pore size of 14 ± 2 nm (Fig. 1c).

The presence of three metals in the Cu-Ag-Au trimetallic bowl-shaped nanocrystals was again confirmed by elemental mapping measurement using high angle annular dark field (HAADF) images. Fig. 2a depicts the HAADF image taken in a carbon coated Au TEM grid (EMS300-Au; 180905) and the corresponding elemental mappings are shown in Fig. 2(b and c) for Ag and Cu, respectively. Similarly, the picture taken in a carbon coated Cu TEM grid (TP300-Cu; 250810-813F) are shown in Fig. 2d and the corresponding elemental mapping confirmed the presence of Au and Ag (Fig. 2(e and f), respectively). HAADF-STEM energy-dispersive X-ray spectroscopy (EDS) for elements Au, Cu and Ag were shown in the supporting information (Fig. S1). From the HAADF-STEM EDS analysis, the approximate atomic ratio of Cu, Ag, and Au were found to be 8:2:1.

Fig. 3a shows high-resolution TEM image of the pore of a single Cu-Ag-Au trimetallic nanobowl. The lattice space value (d-value) obtained from its selected area in the fast Fourier transform (FFT) pattern was 2.25 Å (Fig. 3(b and c)), which corresponds to the lattice planes of cubic Ag (1 1 1); this may be due to the higher Ag content observed compared to Au. The deviation from silver d-spacing of 2.35 Å (1 1 1) is expected here as the other metals (Cu and Au) are alloyed in the same crystal. Notably, the d-spacing values of 2.38 and 2.15 Å for cubic Au and Cu nanocrystal (1 1 1) planes, respectively, are difficult to identify simultaneously.

To further confirm the TEM results and obtain information regarding the crystalline structure and crystal phase of trimetallic

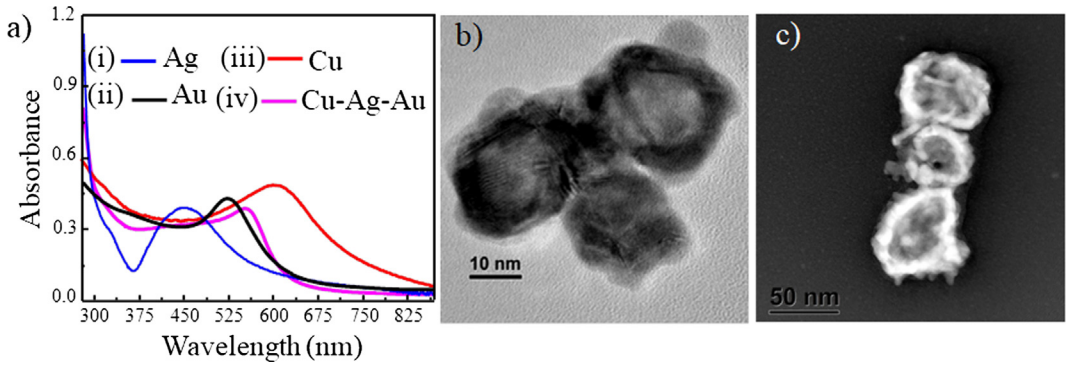

Fig. 1. (a) Absorption spectra of Ag (i), Au (ii), Cu(iii) and (iv) bowls-like Cu-Ag-Au trimetallic nanocrystals, respectively. (b) Corresponding TEM images of Cu-Ag-Au trimetallic nanostructure. And (c) represents the inverted TEM images which show 3D structure of trimetallic Cu-Ag-Au nanobowls.

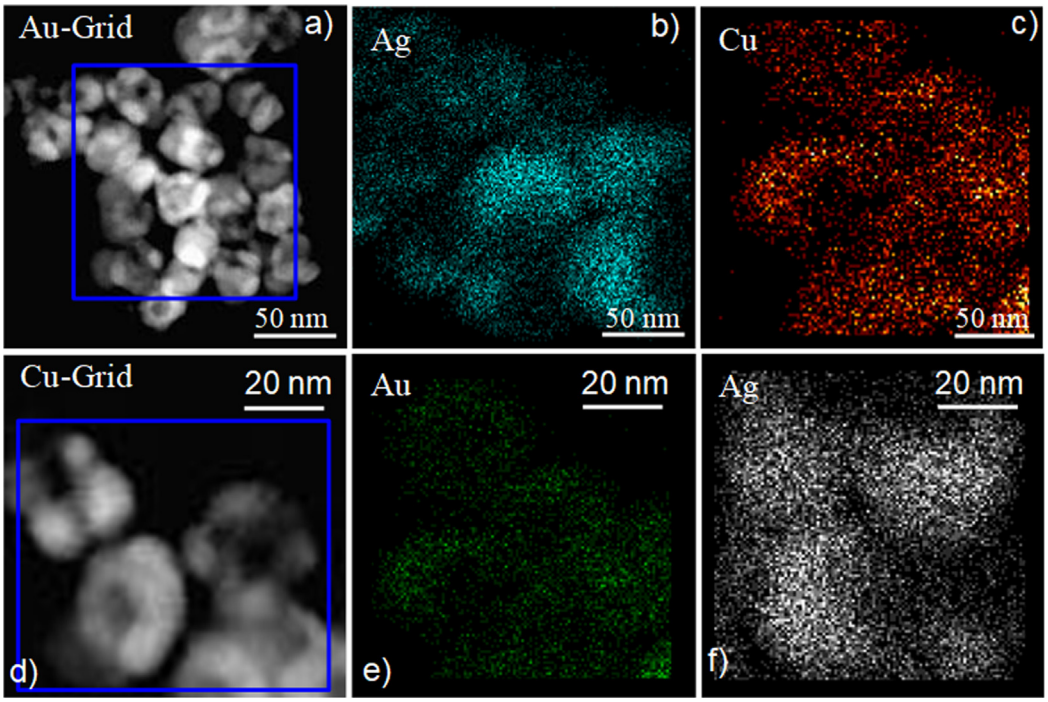

Fig. 2. HAADF-STEM images of (a) Cu-Ag-Au trimetallic nanostructure measured on the Au microscopic grid, (b) and (c) elemental mappings for the elements Ag and Cu respectively. (d) HAADF-STEM image of Cu-Ag-Au trimetallic nanostructure measured on the Cu microscopic grid and (e) and (f) the corresponding elemental mappings for the elements Ag and Au respectively.

Cu-Ag-Au nanobowls, powder X-ray diffraction (XRD) study was carried out. XRD patterns of Cu-Ag-Au trimetallic nanocrystals are shown in Fig. 3d and were found to be consistent with the TEM observations. The sharp diffraction peaks were pointed out for the (1 1 1), (2 0 0), (2 2 0), (3 1 1) and (2 2 2) planes of both Au and Ag components with face centered cubic structure (fcc) (PDF no. 00-004-0784 and PDF no. 01-087-0720, respectively), and the (1 1 1), (2 0 0), (2 2 0) and (3 1 1) planes of Cu component (PDF no. 00-004-0836). Because of the very close lattice spacing match between Au (2.38 Å) and Ag (2.35 Å), their peaks highly imbricate one another and can be tentatively ascribed to the existence of both metals. Consequently, it was very ambitious to isolate both Au and Ag peaks. Based on the XRD analysis results, it is believed that the crystal structures are identical to those of fcc crystals of Cu, Ag, and Au which indicates the existence of all the three metals in the nanocrystals. The Cu-Ag-Au noble trimetallic bowls possessed a highly crystalline structure and no amorphous crystals or peaks of CuO or other oxidation state was observed, which suggested that oxidation of the Cu component is negligible. In comparison with the respective reference cubic metals, the peaks observed here were shifted from the standard metallic states, suggesting that the trimetallic nanobowl is in the alloy form. Thus, the XRD results are in good agreement with the TEM data.

Further, to know the composition of the bowl-like Cu-Ag-Au trimetallic nanostructure, we carried out X-ray photoelectron spectroscopy (XPS) measurement. Fig. 4 depicts the XPS spectra of the Cu-Ag-Au trimetallic nanobowls. The binding energies of the noble metals Ag 3d at 368.2 ± 0.1 eV (Fig. 4a), Cu 2p at 932.8 ± 0.1 eV (Fig. 4b), and Au 4f at 84.1 ± 0.1 eV (Fig. 4c) indicate a metallic state [35–37], i.e., complete reduction of noble metal. The Cu LMM Auger spectrum has a main peak at 573.2 ± 0.1 eV (Fig. S2) and the Auger parameter calculated using the main LMM peak gives a value of 1846.3 ± 0.1 eV, clarifying that the main chemical state of Cu is in the zero valences [38]. This result further confirms the formation of Cu-Ag-Au trimetallic bowls. Interest-

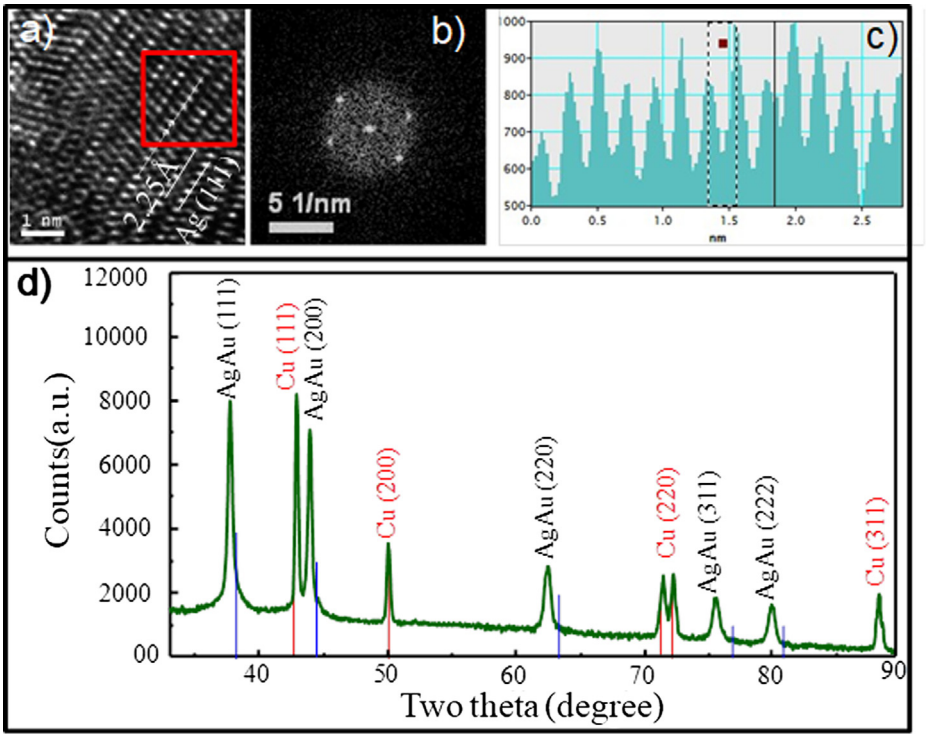

Fig. 3. (a) HRTEM images of single Cu-Ag-Au trimetallic nanobowls, (b) the selected area FFT pattern obtained from the HRTEM image in panel (a) and (c) the corresponding d-profile of Ag in Cu-Ag-Au trimetallic nanobowls. And (d) Powder XRD pattern of the trimetallic nanocubes with standard metal zero states.

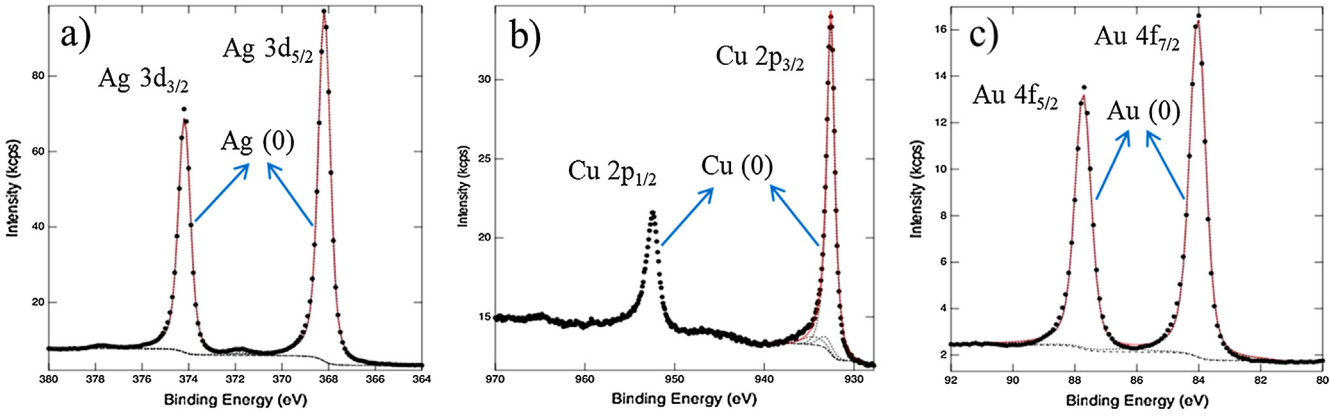

Fig. 4. XPS spectra of (a) Ag 3d and (b) Cu 2p and (c) Au 4f in Cu-Ag-Au trimetallics nanobowls.

ingly, compared to the single metal Cu, Ag and Au, the binding energy of the individual components in the trimetallic nanocrystal showed a slight shift, indicating the changes in the electronic structure due to the charge transfer among Cu, Ag and Au [39,40]. An increase in the binding energy as a function of particle size has been previously reported with Pt-based nanoparticles [43]. Thus, it is reasonable to assume that all the three elements (Cu, Ag, and Au) are uniformly distributed in the bowl-like nanostructure according to their compositions.

The bowl-type trimetallic structure of noble Cu-Ag-Au based nanocrystals was synthesized in an aqueous medium under mild conditions in the presence of ethylene glycol and oleylamine. The yield of the trimetallic Cu-Ag-Au nanobowls could be controlled by adjusting a few synthesis parameters. The formation of heterostructures may be achieved by varying the molar ratio of ethylene glycol and oleylamine from 1:17 to 1:20 while keeping the concentration of Cu, Ag and Au fixed. In order to elucidate the mechanism of Cu-Ag-Au nanocrystal formation and the role each component of the synthesis reaction ($NaBH_4$, ethylenegycol and oleylamine), a series of controlled reactions were carried out. First, we prepared the Cu-Ag bimetallic heterostructure nanocrystals using the same method without the addition of Au(I) precursor (Supplementary Fig. S3a) and this bimetallic heterostructure was confirmed by XPS study (Supplementary Fig. S3b and c). However, there was no nanocrystal formation when the synthesis reaction was performed in the absence of $NaBH_4$. It is believed that $NaBH_4$ reduces Cu (II) to metallic Cu (0) which could have a direct effect on the catalytic activity of upcoming attachments of Ag and Au. In the absence of Ag and Au precursors, under similar reaction conditions, Cu nanocrystals with spherical shape were formed (Supplementary Fig. S4). Thus, addition of $NaBH_4$ is preferred as it initially helps to form separate Cu nanoparticles which act as a seed for further nucleation of Ag and Au. It has been previously reported that ethylene glycol can efficiently be adsorbed on the

Cu (1 1 1) facet [41,42] and to affect the final shape of the aeolotropic interactions between the solid solution and ethylene glycol [43]. Therefore, in order to understand the influence of ethylene glycol on the shape of Cu-Ag-Au nanocrystals, we performed the synthesis reaction in the absence of ethylene glycol, keeping all other conditions the same. However, no hollow or bowl-like nanostructures were observed in the absence of ethylene glycol (Supplementary Fig. S5). This observation clearly demonstrates that ethylene glycol plays a crucial role in the formation of the bowl-like nanostructures [44]. To know the function of oleylamine, we performed the synthesis reaction under similar conditions without oleylamine and observed anisotropic Cu-Ag bimetallic nanocrystals (Supplementary Fig. S6). This is because oleylamine serves both as a reducing and a stabilizing agent [45,46]. Also, attempts for nucleation of Cu-Ag-Au trimetallic bowls in the absence of Cu resulted in the formation of separate Ag (above 80%) and Au nanocrystals (Supplementary Fig. S7). This result indicates that the formation of Cu seed controls the formation of bowl-like Cu-Ag-Au trimetallic nanocrystals. We assume that slight lattice mismatch and similar crystal structures of the depositing metals assist in multifunctional nanobowls formation.

3.2. Catalytic properties

Reduction of aromatic nitro compounds to the corresponding amine is a fundamental reaction because many amine compounds are used in pharmaceuticals [47], agrochemicals and also amine compounds are useful in polymer chemistry [48] and material science [49]. Due to this widespread application, development of mild and efficient methods to reduce the nitro compound is of great significance. However, aromatic nitro compounds are not reduced without a catalyst by metal boron hydrides (i.e., $NaBH_4$) in aqueous solution. It is well known that noble metals like Cu, Au, Pt, and Pd are found to be more active catalysts compared to other metal, non-noble or metal oxides for reduction of 4-NP to 4-AP in the presence of $NaBH_4$. Owing to the high cost and insufficiency of noble metals, few trimetallic alloys have been developed [50,51]. However, to the best of our knowledge, there are still no reports on noble trimetallic alloys used for 4-NP to 4-AP reduction. To explore the catalytic properties of the bowl-like Cu-Ag-Au trimetallic nanostructures prepared in this study, we performed 4-nitrophenol to 4-aminophenol reduction at room-temperature in the presence of Cu-Au-Ag nanobowls or its constituent Cu, Au and Ag nanoparticles. The progress of the reduction reaction was monitored by UV–vis spectrophotometer. To optimise the reduction reaction in presence of Cu-Ag-Au nanobowl catalyst, a series of the controlled reactions were carried out. Fig. 5 shows the UV–vis spectra for the reduction of 4-nitrophenol to 4-aminophenol after the addition of catalyst Cu-Au-Ag nanobowls to the reaction mixture containing 4-NP and $NaBH_4$. The UV–Vis spectra were taken at a time (t) interval of 0.5 min. Aqueous solution of 4-NP has an absorption maxima at 317 nm, but in the $NaBH_4$ medium (pH~13) this peak was shifted to 400 nm due to the formation of 4-nitrophenolate ion. It is noteworthy to mention that the intensity of the maximum absorption of 4-NP at 400 nm did not change over time even after the mixing of superfluous $NaBH_4$ solution. It confirmed that the reduction reaction did not proceed by aqueous $NaBH_4$ solution without addition of a catalyst [52,53]. With the addition of the catalyst Cu-Au-Ag nanobowls to the reaction mixture containing 4-NP and $NaBH_4$, a gradual decrease in the characteristic absorption peak of 4-nitrophenol at 400 nm and an augmentation of a new peak for 4-aminophenol at 298 nm is observed (Fig. 5a). It is also observed that within 7 min, the intensity of the absorption peak of 4-NP at 400 nm almost vanishes to zero, which indicates the completion of the reduction of 4-NP. Hence, the catalytic efficiency of the reduction

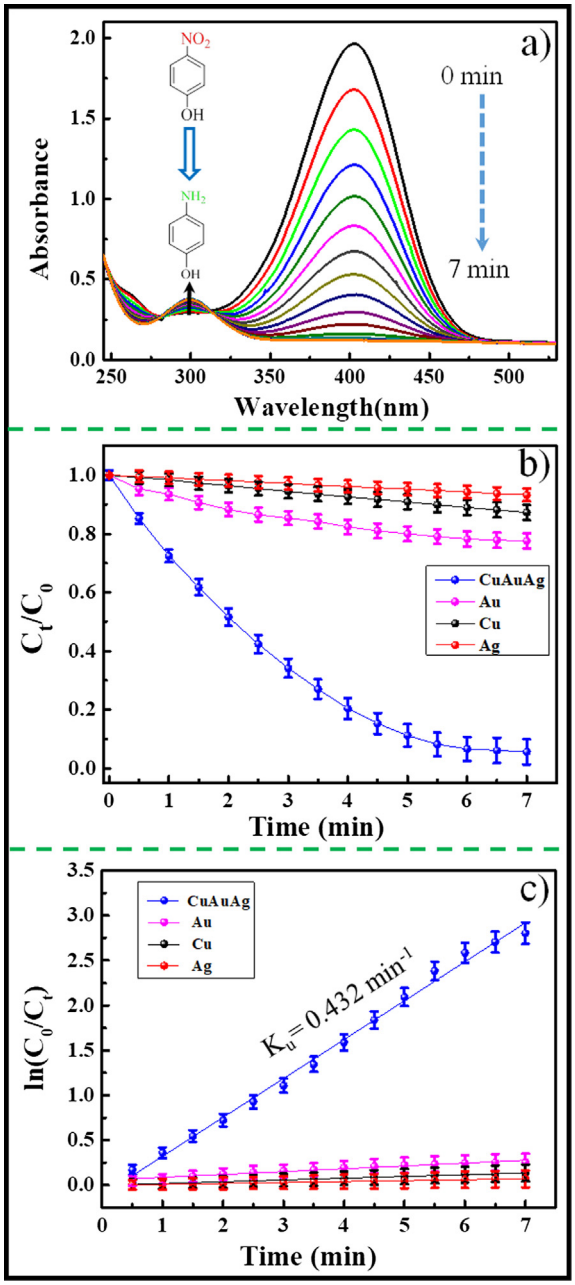

Fig. 5. (a) UV–vis spectra of 4-NP reduced by $NaBH_4$ in the presence of CuAgAu nanobowls with 0.5 min time interval; (b) reduction of 4-NP to 4-AP by in presence of CuAgAu nanobowls, Au, Cu and Ag nanoparticles; (c) $\ln(C_0/C_t)$ vs t plot for determination of apparent rate constants of nanobowls and its constituent nanoparticles [the error bars represent 5% standard deviations].

reaction is 98.6% in presence of Cu-Au-Ag nanobowls. It has also been observed that there was minimal change in the absorption peak of 4-NP in presence of pure Ag, Cu and Au nanoparticles and the corresponding catalytic efficiencies were 6.7%, 13.4% and 22.7%, respectively (Supplementary Fig. S8). The catalytic rate of the reduction reaction was determined from the following equation,

$$K_r = (A_0 - A_t)/A_t \quad (1)$$

where A_0 and A_t are the initial absorbance and the absorbance at time t, respectively.

The kinetic profile of the catalytic reduction reaction showed apparent first-order kinetics which can be expressed as

$$\ln(C_0/C_t) = k_u t$$

where k_u is the apparent reaction rate constant, C_0 is the concentration of 4-NP at time zero, and C_t is the concentration of 4-NP at different time intervals.

A linear relationship between $\ln(C_0/C_t)$ and t (Fig. 5c) reinforces the apparent first-order kinetics of 4-NP to 4-AP reduction reaction. From Fig. 5c, the rate constants of 4-NP to 4-AP reduction reactions were found to be 0.432, 0.032, 0.019 and 0.01 min^{-1} for Cu-Au-Ag nanobowls, Au, Cu, and Ag nanoparticles, respectively. Thus, the trimetallic nanobowls are 14, 23 and 43 fold more active than the individual constituents Au, Cu and Ag, respectively. This result suggests that the formation of trimetallic Cu-Ag-Au nanobowls enhance reactivity, probably due to the modulation of electronic structure. For better interpretation of the catalytic activity, electrochemical impedance spectroscopic (EIS) investigations of all four catalysts were performed under identical experimental conditions. It is clear from the EIS study results that the formation of bowl-like Cu-Ag-Au trimetallic hybrid nanostructures enhances the reduction kinetics (Supplementary Fig. S9). Overall, the bowl-like Cu-Ag-Au trimetallic nanostructures show superior catalysis among the four catalysts. This can be explained by considering the inconsistent structure of nanomaterials which drives the divergent charge transfer rates on the surface [54]. Further, the reduction rate was found to be much higher compared to several recently reported mono/bimetallic systems composed of Cu, Ag and Au (Table S1). In this trimetallic nanostructure, the triple homogeneous mixture may introduce remarkable imperfection on the nanobowls surface and revise the inter-atomic distances because of lattice strain initiated from ternary defects. This may generate more active sites and tune the energy levels of bonding electrons to boost up the catalytic efficiency of the trimetallic nanobowls [55]. Moreover, the modification of electronic structure of the three metallic components might be another crucial aspect for improving catalytic activity. Therefore, the increased catalytic activity of trimetallic nanocatalyst Cu-Ag-Au alloy is dependent upon the formation of the bowl-like structure which results in efficient reduction of 4-NP to 4-AP.

4. Conclusions

In summary, we report the synthesis of Cu-Ag-Au noble trimetallic nanocrystals from plasmonic Ag, Cu and Au, with a unique bowl-like structure. In almost all synthesized nanocrystals, the three components, Cu, Ag, and Au, were combined to form hollow and bowl-like nanostructures. Such trimetallic bowl-like Cu-Ag-Au nanostructures have not been explored previously for the reduction of 4-NP to 4-AP. The Cu-Ag-Au noble trimetallic nanocrystals show maximum efficiency of 98.6% for the reduction of 4-NP to 4-AP which is 14, 23 and 43 fold more active than the constituent metals Au, Cu and Ag, respectively. Thus, the Cu-Ag-Au nanobowls synthesised in this study show superior catalysis for the model reduction reaction compared to its constituent metals and a higher reduction rate compared with other recently reported mono/bimetallic systems composed of Cu, Ag and Au. We are carrying out further work for developing new Cu-Ag-Au noble trimetallic nanostructure-based electrocatalysts for photoelectrochemical cells.

Acknowledgements

The Department of Science and Technology (DST; Project No. EEQ/2017/000467) provided financial support for this work and is gratefully acknowledged. We acknowledge the Ota Nano-microscopyCenter (Aalto-NMC) at Aalto University, Finland, for providing the facilities for carrying out XPS experiments. We also acknowledge Indian Association for the Cultivation of Science, Kolkata, India for providing the UHR-FEG-TEM facilities. Authors thank Jyothi Ramanathan, PhD (Professional Scientific Writer) for writing and editing services. All authors contributed to the development of the manuscript, reviewed and approved the final version of the paper.

Appendix A. Supplementary material

Supplementary data to this article can be found online at https://doi.org/10.1016/j.jcis.2019.08.047.

References

[1] J. Huang et al., Ag dendrite-based Au/Ag bimetallic nanostructures with strongly enhanced catalytic activity, Langmuir 25 (19) (2009) 11890–11896.
[2] Y. Mizukoshi et al., Characterization and catalytic activity of core-shell structured gold/palladium bimetallic nanoparticles synthesized by the sonochemical method, J. Phys. Chem. B 104 (25) (2000) 6028–6032.
[3] N. Nishida et al., Fabrication of liquid crystal sol containing capped Ag-Pd bimetallic nanoparticles and their electro-optic properties, J. Phys. Chem. C 112 (51) (2008) 20284–20290.
[4] Y.-S. Shon et al., Monolayer-protected bimetal cluster synthesis by core metal galvanic exchange reaction, Langmuir 18 (10) (2002) 3880–3885.
[5] K.K. Haldar, S. Kundu, A. Patra, Core-size-dependent catalytic properties of bimetallic Au/Ag core-shell nanoparticles, ACS Appl. Mater. Interfaces 6 (24) (2014) 21946–21953.
[6] K.K. Haldar et al., Au/CdSe hybrid nanoflowers: a high photocurrent generating photoelectrochemical cells, Gold Bull. (2019) 1–7.
[7] S.K. Ghosh et al., Bimetallic Pt–Ni nanoparticles can catalyze reduction of aromatic nitro compounds by sodium borohydride in aqueous solution, Appl. Catal. A: General 268 (1–2) (2004) 61–66.
[8] M. Sanyal, U. Sharma, Selective reduction of nitro group using CuNi bimetallic nanoparticles, SN Appl. Sci. 1 (4) (2019) 353.
[9] R. Ferrando, J. Jellinek, R.L. Johnston, Nanoalloys: from theory to applications of alloy clusters and nanoparticles, Chem. Rev. (Washington, DC, U. S.) 108 (3) (2008) 845–910.
[10] L. Sun et al., Multifaceted gold-palladium bimetallic nanorods and their geometric, compositional, and catalytic tunabilities, ACS Nano 11 (3) (2017) 3213–3228.
[11] R. Liu et al., Alloyed crystalline Au-Ag hollow nanostructures with high chemical stability and catalytic performance, ACS Appl. Mater. Interfaces 8 (26) (2016) 16833–16844.
[12] H. Ataee-Esfahani et al., Synthesis of bimetallic Au@Pt nanoparticles with Au core and nanostructured Pt shell toward highly active electrocatalysts, Chem. Mater. 22 (23) (2010) 6310–6318.
[13] Q. Shi et al., A facile method for synthesizing dendritic core-shell structured ternary metallic aerogels and their enhanced electrochemical performances, Chem. Mater. 28 (21) (2016) 7928–7934.
[14] S. Zhou et al., Enhanced CO tolerance for hydrogen activation in Au-Pt dendritic heteroaggregate nanostructures, J. Am. Chem. Soc. 128 (6) (2006) 1780–1781.
[15] Y. Hu et al., Bimetallic Pt-Au nanocatalysts electrochemically deposited on graphene and their electrocatalytic characteristics towards oxygen reduction and methanol oxidation, Phys. Chem. Chem. Phys. 13 (9) (2011) 4083–4094.
[16] Z. Peng, H. Yang, PtAu bimetallic heteronanostructures made by post-synthesis modification of Pt-on-Au nanoparticles, Nano Res. 2 (5) (2009) 406–415.
[17] M. Tsuji et al., Preparation of Cu@Ag core-shell nanoparticles using a two-step polyol process under bubbling of N2 gas, Chem. Lett. 38 (6) (2009) 518–519.
[18] R.G. Weiner, S.E. Skrabalak, Seed-mediated co-reduction as a route to shape-controlled trimetallic nanocrystals, Chem. Mater. 28 (12) (2016) 4139–4142.
[19] B.K. Patra et al., Monodisperse AuCuSn trimetallic nanocube catalysts, Chem. Commun. (Cambridge, U. K.) 52 (8) (2016) 1614–1617.
[20] X. Sun et al., Core/shell Au/CuPt nanoparticles and their dual electrocatalysis for both reduction and oxidation reactions, J. Am. Chem. Soc. 136 (15) (2014) 5745–5749.
[21] S. Jing, X. Guo, Y. Tan, Branched Pd and Pd-based trimetallic nanocrystals with highly open structures for methanol electrooxidation, J. Mater. Chem. A 4 (20) (2016) 7950–7961.
[22] J. Mao et al., A facile strategy for the synthesis of branched Pt-Pd-M (M = Co, Ni) trimetallic nanocrystals, CrystEngComm 18 (22) (2016) 4023–4026.
[23] X. Liu et al., Au-Cu alloy nanoparticles supported on silica gel as catalyst for CO oxidation: effects of Au/Cu ratios, Catal. Today 160 (1) (2011) 103–108.
[24] W. Li et al., Silica-supported Au-Cu alloy nanoparticles as an efficient catalyst for selective oxidation of alcohols, Appl. Catal., A 433–434 (2012) 146–151.
[25] K. Chatterjee et al., Static and in situ TEM investigation of phase relationships, phase dissolution, and interface motion in Ag-Au-Cu alloy nanoparticles, Acta Mater. 52 (10) (2004) 2923–2935.
[26] T. Pasini et al., Selective oxidation of 5-hydroxymethyl-2-furfural using supported gold-copper nanoparticles, Green Chem. 13 (8) (2011) 2091–2099.

[27] S.S. Shankar et al., Rapid synthesis of Au, Ag, and bimetallic Au core–Ag shell nanoparticles using Neem (Azadirachta indica) leaf broth, J. Colloid Interf. Sci. 275 (2) (2004) 496–502.
[28] K.K. Haldar et al., Photophysical properties of Au-CdTe hybrid nanostructures of varying sizes and shapes, ChemPhysChem 13 (17) (2012) 3989–3996.
[29] K.K. Haldar, T. Sen, A. Patra, Au@ ZnO core– shell nanoparticles are efficient energy acceptors with organic dye donors, J. Phys. Chem. C 112 (31) (2008) 11650–11656.
[30] M. Tsuji et al., Synthesis of bicompartmental Ag/Cu nanoparticles using a two-step polyol process, Chem. Lett. 38 (8) (2009) 860–861.
[31] M. Tsuji et al., Synthesis of Ag@Cu core-shell nanoparticles in high yield using a polyol method, Chem. Lett. 39 (4) (2010) 334–336.
[32] I. Pastoriza-Santos et al., Aerobic synthesis of Cu nanoplates with intense plasmon resonances, Small 5 (4) (2009) 440–443.
[33] G. Panzner, B. Egert, H.P. Schmidt, The stability of cupric oxide and cuprous oxide surfaces during argon sputtering studied by XPS and AES, Surf. Sci. 151 (2–3) (1985) 400–408.
[34] M. Tsuji et al., Epitaxial growth of Au@Cu core-shell nanocrystals prepared using the PVP-assisted polyol reduction method, Cryst. Growth Des. 10 (12) (2010) 5129–5135.
[35] K.K. Haldar et al., Hybrid colloidal Au-CdSe pentapod heterostructures synthesis and their photocatalytic properties, ACS Appl. Mater. Interfaces 4 (11) (2012) 6266–6272.
[36] K.K. Haldar et al., One-pot synthesis of Au embedded ZnO nanorods composite heterostructures with excellent photocatalytic properties, ChemistrySelect 3 (27) (2018) 7882–7890.
[37] N. Feng et al., Understanding the high photocatalytic activity of (B, Ag)-codoped TiO2 under solar-light irradiation with XPS, solid-state NMR, and DFT calculations, J. Am. Chem. Soc. 135 (4) (2013) 1607–1616.
[38] M.T. Nguyen et al., Au/Cu bimetallic nanoparticles via double-target sputtering onto a liquid polymer, Langmuir 33 (43) (2017) 12389–12397.
[39] X. Hong et al., AuAg nanosheets assembled from ultrathin AuAg nanowires, J. Am. Chem. Soc. 137 (4) (2015) 1444–1447.
[40] D. Kim et al., Synergistic geometric and electronic effects for electrochemical reduction of carbon dioxide using gold-copper bimetallic nanoparticles, Nat. Commun. 5 (2014) 4948.
[41] M. Tsuji et al., Shape-dependent evolution of Au@Ag core-shell nanocrystals by PVP-assisted N,N-dimethylformamide reduction, Cryst. Growth Des. 8 (7) (2008) 2528–2536.
[42] Y. Xia et al., Shape-controlled synthesis of metal nanocrystals: simple chemistry meets complex physics?, Angew Chem., Int. Ed. 48 (1) (2009) 60–103.
[43] M. Tsuji et al., Crystal structures and growth mechanisms of Au@Ag core-shell nanoparticles prepared by the microwave-polyol method, Cryst. Growth Des. 6 (8) (2006) 1801–1807.
[44] M. Tsuji et al., Synthesis of Au@Ag@Cu trimetallic nanocrystals using three-step reduction, CrystEngComm 15 (7) (2013) 1345–1351.
[45] S.E. Habas, P. Yang, T. Mokari, Selective growth of metal and binary metal tips on CdS nanorods, J. Am. Chem. Soc. 130 (11) (2008) 3294–3295.
[46] C. Wang et al., Ultrathin Au nanowires and their transport properties, J. Am. Chem. Soc. 130 (28) (2008) 8902–8903.
[47] K.E. Pinkston, D.L. Sedlak, Transformation of aromatic ether-and amine-containing pharmaceuticals during chlorine disinfection, Environ. Sci. Technol. 38 (14) (2004) 4019–4025.
[48] T. Hagiwara, T. Demura, K. Iwata, Synthesis and properties of electrically conducting polymers from aromatic amines, Synth. Met. 18 (1–3) (1987) 317–322.
[49] Y. Sun, S.R. Wilson, D.I. Schuster, High dissolution and strong light emission of carbon nanotubes in aromatic amine solvents, J. Am. Chem. Soc. 123 (22) (2001) 5348–5349.
[50] S. Singh, P. Srivastava, G. Singh, Synthesis, characterization of Co-Ni-Cu trimetallic alloy nanocrystals and their catalytic properties, Part – 91, J. Alloys Compd. 562 (2013) 150–155.
[51] T. Matsushita et al., Synthesis and catalysis of polymer-protected Pd/Ag/Rh trimetallic nanoparticles with a core-shell structure, Bull. Chem. Soc. Jpn. 80 (6) (2007) 1217–1225.
[52] N. Pradhan, A. Pal, T. Pal, Silver nanoparticle catalyzed reduction of aromatic nitro compounds, Colloids Surf. A: Physicochem. Eng. Aspects 196 (2–3) (2002) 247–257.
[53] N. Pradhan, A. Pal, T. Pal, Catalytic reduction of aromatic nitro compounds by coinage metal nanoparticles, Langmuir 17 (5) (2001) 1800–1802.
[54] J. Pei et al., Ir-Cu nanoframes: one-pot synthesis and efficient electrocatalysts for oxygen evolution reaction, Chem. Commun. (Cambridge, U. K.) 52 (19) (2016) 3793–3796.
[55] H. Xu et al., Surface-plasmon-enhanced photo-electrocatalytic ethylene glycol oxidation based on highly open AuAg nanobowls, ACS Sustain. Chem. Eng. 6 (3) (2018) 4138–4146.